Journal of Materials Science and Chemical Engineering, 2016, 4, 51-65
Published Online June 2016 in SciRes. http://www.scirp.org/journal/msce
http://dx.doi.org/10.4236/msce.2016.46007

Scientific Research Publishing

An Experimental Investigation into the Amalgamated Al_2O_3-40% TiO_2 Atmospheric Plasma Spray Coating Process on EN24 Substrate and Parameter Optimization Using TLBO

Thankam Sreekumar Rajesh*, Ravipudi Venkata Rao

S. V. National Institute of Technology Ichchanath, Surat, India
Email: *rajeshtsreekumar@gmail.com

Received 25 April 2016; accepted 27 June 2016; published 30 June 2016

Abstract

Surface coating is a critical procedure in the case of maintenance engineering. Ceramic coating of the wear areas is of the best practice which substantially enhances the Mean Time between Failure (MTBF). EN24 is a commercial grade alloy which is used for various industrial applications like sleeves, nuts, bolts, shafts, etc. EN24 is having comparatively low corrosion resistance, and ceramic coating of the wear and corroding areas of such parts is a best followed practice which highly improves the frequent failures. The coating quality mainly depends on the coating thickness, surface roughness and coating hardness which finally decides the operability. This paper describes an experimental investigation to effectively optimize the Atmospheric Plasma Spray process input parameters of Al_2O_3-40% TiO_2 coatings to get the best quality of coating on EN24 alloy steel substrate. The experiments are conducted with an Orthogonal Array (OA) design of experiments (DoE). In the current experiment, critical input parameters are considered and some of the vital output parameters are monitored accordingly and separate mathematical models are generated using regression analysis. The Analytic Hierarchy Process (AHP) method is used to generate weights for the individual objective functions and based on that, a combined objective function is made. An advanced optimization method, Teaching-Learning-Based Optimization algorithm (TLBO), is practically utilized to the combined objective function to optimize the values of input parameters to get the best output parameters. Confirmation tests are also conducted and their output results are compared with predicted values obtained through mathematical models. The dominating effects of Al_2O_3-40% TiO_2 spray parameters on output parameters: surface rough-

*Corresponding author.

How to cite this paper: Rajesh, T.S. and Rao, R.V. (2016) An Experimental Investigation into the Amalgamated Al_2O_3-40% TiO_2 Atmospheric Plasma Spray Coating Process on EN24 Substrate and Parameter Optimization Using TLBO. *Journal of Materials Science and Chemical Engineering*, **4**, 51-65. http://dx.doi.org/10.4236/msce.2016.46007

ness, coating thickness and coating hardness are discussed in detail. It is concluded that the input parameters variation directly affects the characteristics of output parameters and any number of input as well as output parameters can be easily optimized using the current approach.

Keywords

Atmospheric Plasma Spray (APS), EN24, Design of Experiments (DOE), Teaching Learning Based Optimization (TLBO), Analytic Hierarchy Process (AHP), Al_2O_3-40% TiO_2

1. Introduction

Alumina (Al_2O_3) and Titania (TiO_2) ceramics are popular materials used in plasma spray coating in manufacturing sector. The selection of coating material depends on the application of coating. Alumina is highly corrosion resistant and is used to resist abrasive wear. Al_2O_3-TiO_2 coating is widely known as ceramic coating which shows strong addition to substrate, high dielectric strength, high wear strength and superior protection from corrosion. Ramachandran *et al.* [1] observe that TiO_2 has a lower melting point and it actively combines with alumina grains, which results in to high density. So a coating of Al_2O_3-TiO_2 composite supports the industry to get a hard, wear, oxidation and corrosion resistant coating on the surface of the subtract. EN24 is an alloy steel known as 34CrNiMo6 as per DIN and has Mn up to 0.7% in composition. EN24 is used in components such as gears, shafts, studs and bolts, and its hardness is in the range of 248 to 302 HB. EN24 can be further surface-hardened to create components with enhanced wear resistance by induction, coating or nitriding processing. EN24 possesses low corrosion resistance. An effective coating of Al_2O_3-TiO_2 helps the EN24 steel surface to attain excellent corrosion resistance. A detailed survey of the research studies particularly in the field of Al_2O_3-TiO_2 coatings and EN24 alloy steel applications is carried out in detail.

Yang *et al.* [2] presented the aspects of preparing of nanostructured Al_2O_3-TiO_2-ZrO_2 composite powders and plasma spraying nanostructured composite coating. Forghani *et al.* [3] utilized a design of experiment (DoE) method to identify the effect of air plasma spray (APS) parameters on several main properties of titanium dioxide (TiO_2) coatings. Kang *et al.* [4] studied the influence of contact stress on rolling contact fatigue performance of plasma sprayed Al_2O_3-40% TiO_2 composite ceramic coating using a double-roll test machine. Surface abrasion, spalling, and delamination were observed during this investigation. It was found that the initiation and propagation of fatigue cracks were mainly caused by the shear stress, which was highly influenced by the contact stress. Mishra *et al.* [5] deposited Al_2O_3-13TiO_2 coating on nickel-based Superni 718 and AE 435 super alloys using a low-velocity oxy-fuel (LVOF) process. The coating was characterized for SEM, XRD and surface roughness. The LVOF sprayed Al_2O_3-13TiO_2 coating had shown good oxidation resistance as well as adherence to the substrates under the tested environment.

Bolleddu *et al.* [6] deposited air plasma sprayed nanostructured Al_2O_3-13TiO_2 coatings as a function of critical plasma spray parameter (CPSP), defined as the ratio of arc power to primary gas flow rate, using nitrogen and argon as the primary plasma gases. Effect of CPSP on microstructural and wear characteristics of coatings deposited with nitrogen was found to be relatively small. Morks *et al.* [7] carried out a detailed study of Al_2O_3-50% TiO_2 composite coatings, which were sprayed on a mild steel substrate by using plasma spraying .Yugeswaran *et al.* [8] studied the Critical Plasma Spraying Parameter (CPSP) effect on plasma arc spraying to control the quality of coatings. Palacio *et al.* [9] coated AISI 1040 steel by atmospheric plasma spraying with 13% Al_2O_3 and 45% TiO_2. Micro sized powders (6/22 and 13/41 μm) were used as raw materials for coating. Rico *et al.* [10] compared the mechanical and high temperature wear behavior of Al_2O_3-13% TiO_2 nanostructured coatings to that of the conventional ones. Wang *et al.* [11] prepared Al_2O_3 coatings using supersonic plasma spraying on the porous Si_3N_4 substrate at the spraying power of 52, 54, 58 and 60 kW, respectively. The effect of spraying power on the microstructures and properties of Al_2O_3 coating was investigated. Vargas *et al.* [12] studied evolution of brine permeation in Al_2O_3-TiO_2coatings elaborated by atmospheric plasma spray using Electrochemical Impedance Spectroscopy. Znamirowski *et al.* [13] investigated Titania composite layers made by atmospheric plasma spraying technique and laser engraving Emission characteristics of the emitters made of pure TiO_2 and those made of Al_2O_3-13% TiO_2.Vicent *et al.* [14] deposited Al_2O_3-13% TiO_2 nanostructured and

submicron-nanostructured powders using APS. Optimization of the deposition conditions enabled the reconstituted powders to be successfully deposited, yielding coatings that were well bonded to the substrate.

Murakami *et al.* [15] analysed the complicated fatigue data effects of non-metallic inclusion by adding spherical and angular alumina particles of various controlled sizes on Hard Chrome Coated EN24 Substrate. It was found that the geometrical parameter that controls the scatter of the fatigue strength is the square root of the projection area and not the shape of the inclusions. It is concluded that Fatigue strength of materials containing inclusions larger than a critical size can be predicted.

Ramesh *et al.* [16] studied Fretting wear behaviour of liquid nitrided structural steel, EN24. They had conducted tests at different normal loads on many bearing shaft assemblies and at constant slip amplitude under unlubricated conditions. Coefficient of friction under fretting conditions and wear resistance were measured. Surface chemistry influences the fretting wear behavior more than the hardness of the materials in the case of EN24. Sarmah*et al.* [17] investigated the wear mechanisms while machining EN24 steel having multiple coatings of TiC, Ti (C, N), TiN and AlON. It was concluded that the AlON coatings provide the best crater wear resistance under high speed cutting conditions for EN24. Tomlinson *et al.* [18] analysed running in wear of whiter layers formed on EN24 Steel by centerless grinding. The white layers increased the resistance of the steel to wear. The mechanism of wear was by abrasion and the results followed a simple truncation model.

Aparnadevi *et al.* [19] carried out a study which deals with an objective to implement different heat treatments such as annealing, normalizing and hardening with different quenchants (water and oil) to witness its effect on corrosion behaviour of selected EN8 and EN24 grades of steels. Normalizing, oil quenching and water quenching exhibit lesser degree of corrosion resistance compared to that of annealed specimen. EN24 grade of steel exhibited better corrosion resistance than EN8. Sabithaghosh *et al.* [20] studied the effect of various heat treatments on the mechanical properties of EN24 steel. Ball Indentation Technique has been used to evaluate the variation in mechanical properties due to heat treatment on EN24 steel. Increments in tempering temperature have softened the EN24 steel substrate and thus decreased the strength but increased strain hardening exponent. They reported some typical complicated aspects of the effects of non-metallic inclusions on the fatigue strength.

Mohandas *et al.* [21] Studied the Surface Integrity and Heat Measurement during Hard Turning of Hard Chrome Coated EN24 Substrate. The input parameters considered are spindle speed, feed, depth of cut, nose radius and cutting edge angle. EN24 substrate was coated with hexavalent chrome to a thickness of 170 μm. The surface hardness before and after hard turning of hard chrome plated surfaces were studied. The experimental results revealed that the maximum heat was observed at 2 mm from the cutting edge on the top diagonal.

A number of researchers had explored the effect of various parameters on the final response of atmospheric plasma spray in the last five years. Researchers have utilized DoE methods to different thermal spray processes and for different aspects of this field. Troczynski *et al.* [22] applied response surface methodology (RSM) on plasma spray of WC-12% Co powders to optimize their parameters. Steeper *et al.* [23] used a Taguchi method to study the effects of plasma processing conditions on properties of alumina-titania coatings. In another study, Pierlot *et al.* [24] had utilized full factorial designs for their thermal spray work and carried out a review on the design of experiment methodology for thermal spraying. The design of Hadmard matrix and RSM are discussed in detail. Li *et al.* [25] investigated the plasma spray process parameters with respect to deposition efficiency, porosity and micro hardness using a uniform design of experiment.

It is observed from the thorough literature review that work carried out on EN24 is very rare. The research was mostly related to heat treatment and case hardening. The method followed by many of the researchers globally to relate input parameters to output parameters is through different types of mathematical modeling. But very few attempts are made to create mathematical models to depict the relationships between the input and output parameters in the case of Al_2O_3-TiO_2 coatings. The literature review clearly shows the need for a detailed study for the input parameter optimization of plasma spraying of Al_2O_3-TiO_2 coatings with various weight% of TiO_2 on different metal substrates. The modern optimization techniques applied in the current work are very effective to set appropriate process parameters on plasma spraying machines as it is a very critical step to ensure highest utilization of the resources with no compromise on quality as well as productivity.

2. Experimental Procedure, Preparation and Testing of Al_2O_3-40%TiO_2 Coating

EN24 alloy steel is made with a dimension of 27 mm diameter and 3 mm thickness from a flat sheet using punching process to make test substrate sample pieces. Three samples are used to conduct each of the experi-

ment, assembled in one cartridge. Al_2O_3-40%TiO_2 in powder form supplied by H. C. Starck, USA is used for coating. Thorough sand blasting is carried out on all the samples to keep the sample surface active and clean for coating. Fused Alumina of grit size 60 µm is used as the sand blasting material. This is supplied by Carborundum Universal. Al_2O_3-40% TiO_2 powder is deposited on the rotating substrates by using an SG 100 Plasma spray gun, supplied by Metco. The coating powder is preheated up to 110˚C to ensure the removal of moisture.

The experiments are conducted as per the design of experiments. The details of DoE are shown in **Table 2**. Some of the parameter values, which are kept constant during the entire experiment, are given below.

Spray nozzle	GP, 5.43 mm
Grit blasting pressure	2 Kg/cm^2
Substrate exposure to gun	30 Sec
Primary gas pressure	100 Psi
Secondary gas pressure	80 Psi

Once the coating process is over, the sample pieces are washed in ethanol and dried to avoid accumulation of moisture. Measurement of coating thickness is done with an ultrasonic thickness gauge. The surface roughness values are measured by surface roughness tester SV-C3100 by Mitutoyo Japan. The measurement is done on the coating surface for a length of 15 mm with a pitch of 0.001 mm and scanning speed was 2.0 mm/sec. Hardness tester make Equotip 3, with range of up to 1000 HV is used for hardness measurement

2.1. Experimental Design and Procedure

The experiment is carried out using L_{18} orthogonal array of Taguchi's design of experiments (DoE). Selected responses in this study are surface roughness, coating thickness and hardness. The input parameters considered are distance of plasma spray gun, substrate rpm, arc current, coating power flow rate and carrier gas flow. The entire input parameters considered for the experiment along with levels decided are shown in **Table 1**.

The Design of Experiments is given in detail in **Table 2**.

2.2. Coating Output Parameter Details

The mean values of the measured coating thickness, roughness and hardness are given in **Table 3**.

3. Results and Discussion

Regression modelling is done using MS Excel's data analysis capability for each of the output parameters. The derived mathematical models for output parameters are shown below as Equations (1)-(3).

$$\begin{aligned} T, \text{Thickness } \mu\text{m} = {} & 3011.7469 - 22.328 * D - 12.3777 * N - 3.05812 * A - 27.7096 * G + 14.7876 * P \\ & + 0.01635 * D * N - 0.01949 * D * A + 0.3994 * D * G + 0.3600 * D * P + 0.0249 * N * A \\ & - 0.0216 * N * G + 0.0876 * N * P + 0.1331 * A * G - 0.0735 * A * P - 1.3976 * G * P \end{aligned} \quad (1)$$

Table 1. Ranges of parameters.

No	Parameter	Low level	Middle level	High level
1	Spray distance of gun, mm	75	100	125
2	Carrier gas flow, Lit./min.	20	30	50
3	Powder flow rate, Gms./min.	25	35	50
4	RPM of the substrate	150	250	350
5	Arc current, A	350	400	500

Table 2. DoE for conducting the experiments.

Experiment No	Spray distance mm	Substrate rpm	Arc current A	Carrier gas flow Lit./min.	Powder flow rate Gms./min.
1	75	150	300	20	25
2	75	250	400	30	35
3	75	350	500	40	50
4	125	150	300	30	35
5	125	250	400	40	50
6	125	350	500	20	25
7	175	150	400	20	50
8	175	250	500	30	25
9	175	350	300	40	35
10	75	150	500	40	35
11	75	250	300	20	50
12	75	350	400	30	25
13	125	150	400	40	25
14	125	250	500	20	35
15	125	350	300	30	50
16	175	150	500	30	50
17	175	250	300	40	25
18	175	350	400	20	35

Table 3. The values of measured output parameters.

Experiment No	Mean thickness µm	Mean roughness µm	Mean hardness HV
1	321.33	4.56	586.50
2	422.33	4.51	561.67
3	979.33	5.09	539.27
4	264.00	6.17	465.33
5	542.67	4.72	598.33
6	469.33	4.89	588.33
7	89.00	6.41	304.83
8	228.00	4.35	475.50
9	518.00	4.87	592.17
10	578.33	3.89	713.67
11	491.33	4.44	522.83
12	602.33	5.10	579.50
13	552.00	4.82	668.50
14	294.67	4.52	479.17
15	524.33	4.87	562.50
16	95.33	4.37	339.67
17	240.67	4.62	475.50
18	223.67	5.01	462.83

$$R, \text{Roughness } \mu m = 3.72780 + 0.02176 * D - 0.03127 * N - 0.00751 * A + 0.23388 * G + 0.09309 * P - 0.00002 * D * N - 0.00001 * D * A - 0.00106 D * G + 0.00059 * D * P + 0.00007 * N * A + 0.00023 * N * G - 0.00006 * N * P - 0.00018 * A * G - 0.000021 * A * P - 0.00193 * G * P \quad (2)$$

$$H, \text{Hardness HV} = 1670.757 - 14.2722 * D - 5.08633 * N + 0.193375 * A - 5.111087 * G + 4.157886 * P + 0.016719 * D * N - 0.00661 * D * A + 0.185056 * D * G + 0.180369 * D * P + 0.008285 * N * A - 0.03434 * N * G + 0.034592 * N * P + 0.039088 * A * G - 0.05109 * A * P - 0.4395 * G * P \quad (3)$$

where

D = Spray distance,
N = Substrate RPM,
A = Arc Current,
G = Carrier gas flow, and
P = Powder flow rate.

The values of thickness and hardness are considered as beneficial (higher the better) and the values of thickness and hardness are considered as beneficial (lower the better). ANOVA is carried out on each of these models to check the adequacy as shown in **Tables 4-6**.

Table 4. Regression details and ANOVA of thickness model.

Regression statistics thickness model					
Multiple R	0.99562433				
R square	0.99126781				
Adjusted R square	0.92577639				
Standard error	59.2161339				
Observations	18				
ANOVA					
	df	SS	MS	F	Significance F
Regression	15	796118.9	53074.6	15.13584	0.063662262
Residual	2	7013.101	3506.551		
Total	17	803132			

Table 5. Regression details and ANOVA of roughness model.

Regression statistics					
Multiple R	0.97750				
R square	0.95550				
Adjusted R square	0.62179				
Standard error	0.37276				
Observations	18				
ANOVA					
	df	SS	MS	F	Significance F
Regression	15.00000	5.96760	0.39784	2.86322	0.28920
Residual	2.00000	0.27790	0.13895		
Total	17.00000	6.24550			

Table 6. Regression details and ANOVA of hardness model.

Regression statistics					
Multiple R	0.99782				
R square	0.995645				
Adjusted R square	0.962981				
Standard error	19.62166				
Observations	18				
ANOVA					
	df	SS	MS	F	Significance F
Regression	15	176034.1	11735.61	30.48134	0.032205413
Residual	2	770.0192	385.0096		
Total	17	176804.1			

3.1. Confirmation Experiments

Confirmation tests are conducted with five samples .To conduct the test, random values are selected for all input parameters which lies between maximum and minimum levels. The final measurement of all output parameters are taken and shown in **Tables 7-9** along with predicted values obtained using the proposed mathematical models. The % variation between actual and predicted values is also given in tables.

3.2. SN Analysis

Signal-to-noise ratio, or the SN ratio, is calculated for each set of experiments.SN ratio clearly indicates the effect of each input parameter on the desired output parameter. The values of SN ratios are tabulated as shown in **Table 10** for each factor and level. The range ΔR (R = high SN-low SN) of the SN for each input parameter is found out. The larger the R value for an input parameter, the larger the effect that parameter has on the output parameter. That means, the same change in input parameter signal causes a larger effect on the output parameter is considered as most dominating.

SN ratio values for coating thickness are derived for each input parameters. The values are shown in **Table 11**.

Here, the R value clearly shows that spray gun distance has a dominating effect on the coating thickness. The next deciding parameter in the case of coating thickness is rpm of the EN24 substrate. The sequence of significance is shown as rank. Similarly, SN ratio values are calculated for surface roughness for each parameter and level for all the output parameters as shown in **Table 12**. It is found that arc current has a significant effect on the surface roughness. The next dominant parameter in the case of surface roughness is rpm of the substrate. In the case of surface hardness, the spray distance has a significant effect on the coating hardness as shown in **Table 13**. The next dominant parameter in the case of hardness is carrier gas flow. All the effects of input parameters vs SN Ratio means related to coating thickness, roughness and hardness are shown as graphs in **Figures 1-3**.

3.3. Application of Teaching Learning Based Optimization (TLBO)

Teaching-learning-based optimization (TLBO) is applied individually to each of the mathematical models of output parameters given by Equations (1) to (3) to derive the optimum values of output parameters. TLBO—an advanced optimization method—is a teaching-learning process inspired algorithm proposed by Rao *et al.* [26], based on the effect of influence of a teacher on the output of learners in a class. Teacher and learners describes two basic modes of the learning, through teacher (known as teacher phase) and interacting with the other learners (known as learner phase). The algorithm mimics teaching-learning ability of teacher and learners in a class room. The algorithm-specific parameter-less concept of the algorithm is one of the attracting features of this procedure. The algorithm is very simple to use and it has an effective capability to provide the global or near

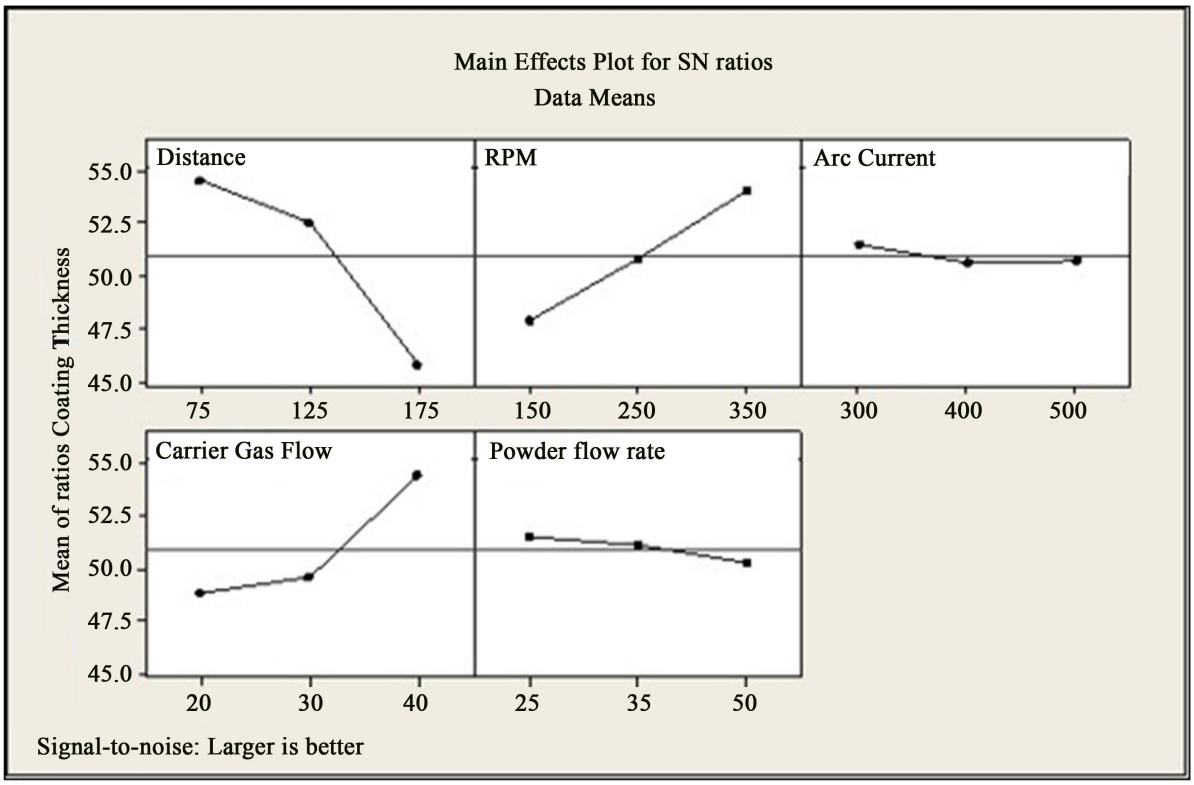

Figure 1. SN ratio vs input parameter in the case of coating thickness.

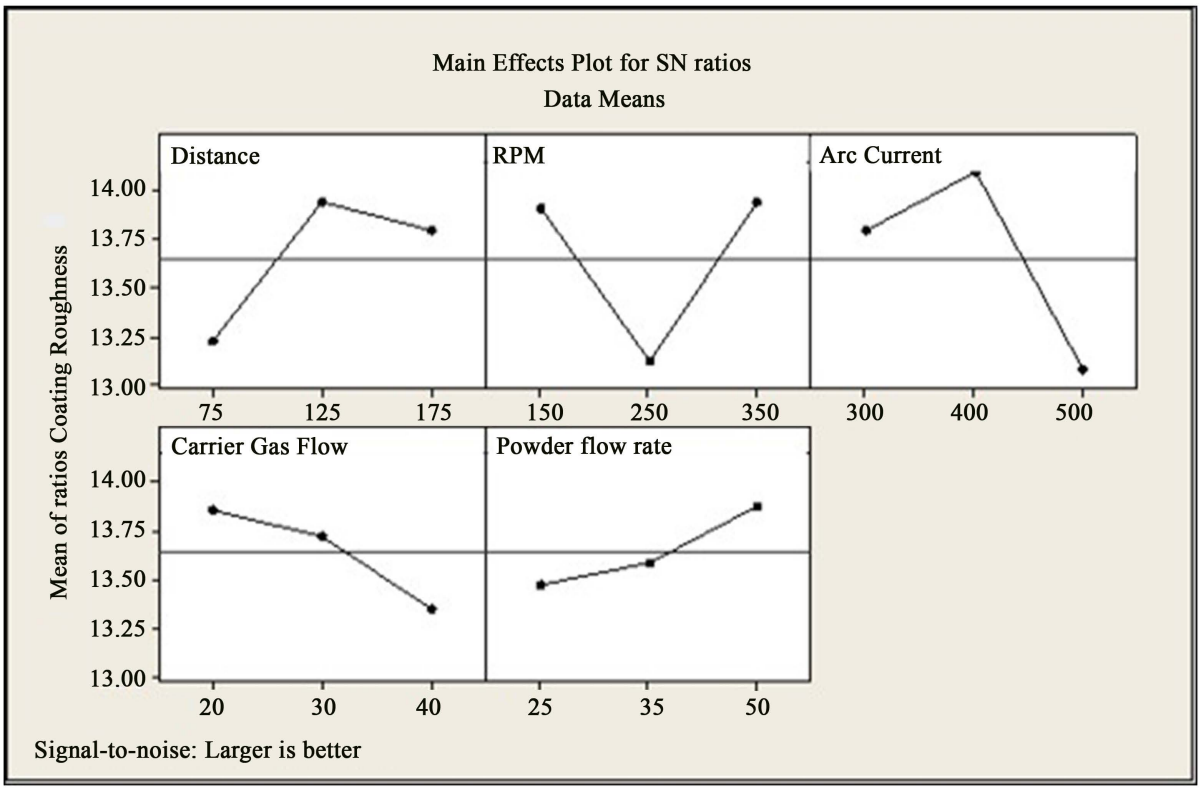

Figure 2. SN ratio vs input parameter in the case of coating roughness.

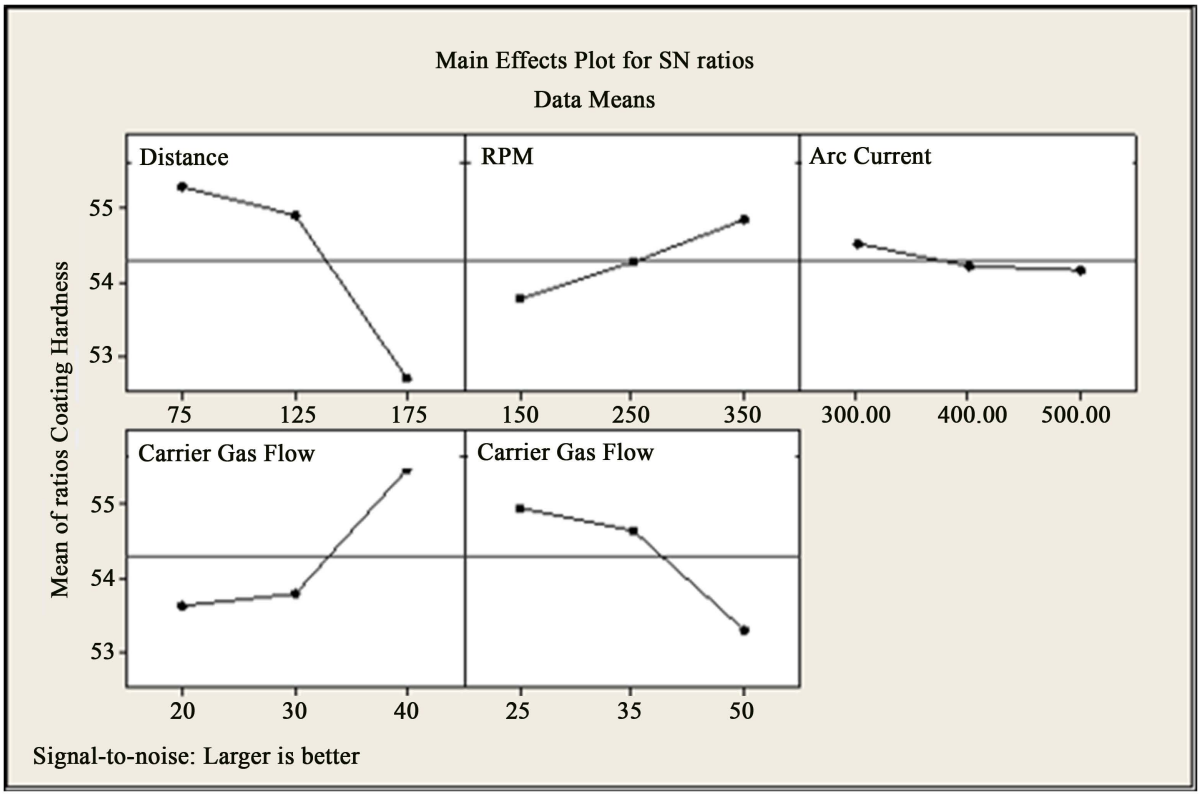

Figure 3. SN ratio vs input parameter in the case of coating hardness.

Table 7. Measured and predicted values—thickness.

Distance mm	Substrate rpm	Current A	Carrier gas flow Lit./Min.	Power flow rate Gms./Min.	Thickness µm	Predicted values µm	% Variation
100	200	350	25	40	312.54	289.00	7.53
90	175	375	35	45	178.32	197.79	10.92
80	190	425	35	40	322.89	358.41	9.91

Table 8. Measured and predicted values—hardness.

Distance mm	Substrate rpm	Current A	Carrier gas flow Lit./Min.	Power flow rate Gms./Min.	Hardness HV	Predicted values HV	% Variation
150	300	450	35	30	431.45	481.31	10.36
160	225	325	25	30	568.42	639.38	12.48
80	190	425	35	40	278.26	285.46	2.52

Table 9. Measured and predicted values—roughness.

Distance mm	Substrate rpm	Current A	Carrier gas flow Lit./Min.	Power flow rate Gms./Min.	Roughness µm	Predicted values µm	% Variation
100	200	350	25	40	3.84	4.35	11.79
150	300	450	35	30	4.54	4.77	5.17
160	225	325	25	30	4.08	4.30	5.06

Table 10. Levels and parameters SN ratio.

Level	P1	P2	P3	P4
1	$SN_{P1,1}$	$SN_{P2,1}$	$SN_{P3,1}$	$SN_{P4,1}$
2	$SN_{P1,2}$	$SN_{P2,2}$	$SN_{P3,2}$	$SN_{P4,2}$
3	$SN_{P1,3}$	$SN_{P2,3}$	$SN_{P3,3}$	$SN_{P4,3}$
Δ R	R_{P1}	R_{P2}	R_{P3}	R_{P4}
Rank	….	….	….	….

Table 11. SN ratio matrix and ΔR values of coating thickness.

	Distance mm	rpm	Current A	Carrier gas flow Lit./Min.	Powder flow rate Gms./Min.
Level 1	54.52	47.87	51.45	48.79	51.47
Level 2	52.53	50.87	50.6	49.61	51.14
Level 3	45.77	54.09	50.77	54.42	50.22
Δ R	8.75	6.21	0.85	5.62	1.25
Rank	1	2	5	3	4

Table 12. SN ratio matrix and ΔR values of coating roughness.

	Distance mm	rpm	Current A	Carrier gas flow Lit./Min.	Powder flow rate Gms./Min.
Level 1	13.22	13.9	13.79	13.86	13.47
Level 2	13.93	13.11	14.08	13.73	13.59
Level 3	13.79	13.93	13.07	13.35	13.88
Δ R	0.71	0.81	1.02	0.5	0.41
Rank	3	2	1	4	5

Table 13. SN ratio matrix and ΔR values of coating hardness.

	Distance mm	rpm	Current A	Carrier gas flow Lit./Min.	Powder flow rate Gms./Min.
Level 1	55.28	53.77	54.51	53.62	54.93
Level 2	54.9	54.27	54.21	53.8	54.63
Level 3	52.69	54.84	54.15	55.46	53.31
Δ R	2.59	1.08	0.37	1.84	1.63
Rank	1	4	5	2	3

global optimum solutions in comparatively less number of function evaluations. More details about the TLBO algorithm can be found in [27] and https://sites.google.com/site/tlborao. Another recently developed algorithm specific parameter-less algorithm known as Jaya [28] may also be attempted for optimization.

Pickard *et al.* [29] mentioned that the TLBO algorithm has origin bias affecting the population convergence and success rates of benchmark objective functions with origin solutions. But they had overlooked the fact that the TLBO algorithm provided better results even for the benchmark functions whose solutions were not located at the origin [27] [30]-[32]. Many researchers had obtained better results with TLBO algorithm for different objective functions with different characteristics. Moreover, the results shown by Pickard *et al.* [29] in **Table 1** of their paper are checked by the first author of this paper under the same conditions and it is found that the results

shown by Pickard *et al.* [29] for non-origin based objective functions were incorrectly reported. The TLBO algorithm has obtained the optimum results irrespective of whether the solution to the objective function is located at the origin or not. Comments were also made by Rao [32] on the unusual concept of function evaluations required for duplicate removal. Furthermore, Pickard *et al.* [29] mentioned that the bias is occurring when teaching factor takes the value of 2. But in the original TLBO algorithm, the value of teaching factor varies randomly during each iteration either as 1 or 2 and it will not remain as 2 during all the iterations and Pickard *et al.* [29] had not considered this fact. The TLBO algorithm has been applied by many researchers to many real life applications (whose solutions are not located at origin) in different engineering disciplines and obtained better results as compared to the other advanced optimization algorithms [32].

In the present work, 30 independent runs with a population size of 10 and 100 number of iteration generations is considered for executing the TLBO algorithm for the optimisation of individual objective functions of output parameters. Optimized values obtained by applying TLBO algorithm for the individual objective functions of output parameters are: T (Thickness), R (Roughness) and H (Hardness) are 1476.0 μm, 4.1659 μm and 915.847 HV respectively. Convergence graphs of TLBO for each of the output parameters are displayed in **Figures 4-6**.

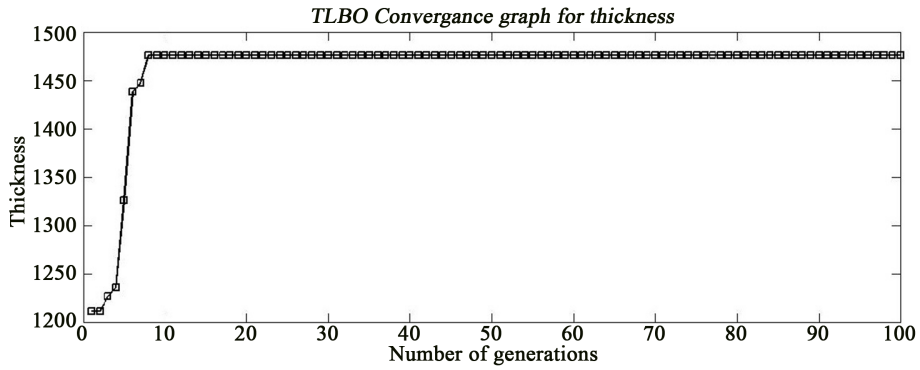

Figure 4. Convergence graph of TLBO for coating thickness.

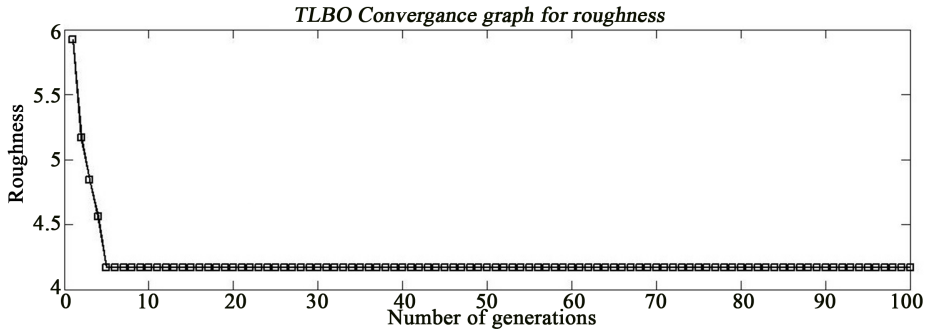

Figure 5. Convergence graph of TLBO for coating roughness.

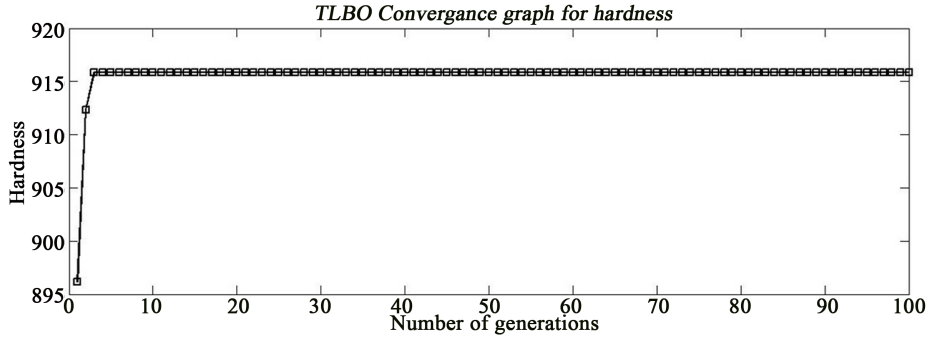

Figure 6. Convergence graph of TLBO for coating hardness.

3.4. Formation of Combined Objective Function

A combined objective function is formed by apirori approach, involving all the three objective functions. The Combined objective function is solved by applying TLBO algorithm for the given ranges of the input parameters. By considering only one objective at a time, the optimized values for individual output parameters *T*, *R* and *H* are already obtained by applying TLBO. However, practically, optimization of all these output parameters is required together simultaneously. That way, the problem becomes a multi-objective problem, as shown in Equation (4).

$$Z_{\max} = W_2 * \frac{T}{T_{\max}} + W_3 * \frac{H}{H_{\max}} - W_1 * \frac{R}{R_{\min}}. \tag{4}$$

In the above Equation (4) $T_{\max}$, $R_{\min}$ and $H_{\max}$ represents the optimum desired values *T*, *R* and *H* when solved individually for the given range of input parameters. These values are 1476.0 μm, 4.1659 μm and 915.847 HV respectively. W_1, W_2 and W_3 show the weights assigned to the individual objective functions. The weights W_1, W_2 and W_3 can be assigned by the researcher based on his experience, literature review and input from other experts. In this paper, a systematic approach of assigning the weights, known as Analytic Hierarchy Process (AHP) [33] is presented. This method lets the person to assign the weights by following the theory of relative importance. The numbers 3, 5, 7, and 9 correspond to the verbal judgments "moderate importance", "strong importance", "very strong importance", and "absolute importance" is given. A parameter compared with itself is assigned the value 1 so, the main diagonal entries of the pair-wise comparison matrix are all 1. Decision making matrix is made as shown below comparing the output parameters, Coating thickness (*T*), Surface roughness (*R*) and Hardness (*H*).

$$A_1 = \begin{array}{c} \text{Criterion} \\ T \\ R \\ H \end{array} \begin{array}{c} \begin{array}{ccc} T & R & H \end{array} \\ \begin{bmatrix} 1 & 1/3 & 1/5 \\ 3 & 1 & 1/3 \\ 5 & 3 & 1 \end{bmatrix} \end{array}$$

The normalized weights of each output parameter is calculated following the procedure and these are W_T = 0.1048, W_R = 0.2583 and W_H = 0.6370. The value of maximum Eigen value ($\lambda_{\max}$) is 3.0385 and consistency ratio (CR) = 0.036712, which is much less than the allowed CR value of 0.1. Thus, there is good consistency in the judgments made. The weights calculated following the AHP method are applied to the combined objective function as given below in Equation (5).

$$\begin{aligned} Z_{\max} = {} & 0.1048/1476.0 * (3011.7469 - 22.328 * D - 12.3777 * N - 3.05812 * A \\ & - 27.7096 * G + 14.7876 * P + 0.01635 * D * N - 0.01949 * D * A \\ & + 0.3994 * D * G + 0.3600 * D * P + 0.0249 * N * A - 0.0216 * N * G \\ & + 0.0876 * N * P + 0.1331 * A * G - 0.0735 * A * P - 1.3976 * G * P) \\ & + 0.6370/915.847 * (1670.757 - 14.2722 * D - 5.08633 * N + 0.193375 * A \\ & - 5.111087 * G + 4.157886 * P + 0.016719 * D * N - 0.00661 * D * A \\ & + 0.185056 * D * G + 0.180369 * D * P + 0.008285 * N * A - 0.03434 * N * G \\ & + 0.034592 * N * P + 0.039088 * A * G - 0.05109 * A * P - 0.4395 * G * P) \\ & - 0.2583/4.1659 * (3.72780 + 0.02176 * D - 0.03127 * N - 0.00751 * A \\ & + 0.23388 * G + 0.09309 * P - 0.00002 * D * N - 0.00001 * D * A \\ & - 0.00106 * D * G + 0.00059 * D * P + 0.00007 * N * A + 0.00023 * N * G \\ & - 0.00006 * N * P - 0.00018 * A * G - 0.000021 * A * P - 0.00193 * G * P) \end{aligned} \tag{5}$$

Now, the TLBO algorithm is used to optimize the combined objective function and the optimum value of coefficient $Z_{\max}$ is achieved. Considering a population of 10 and after 30 independent runs and 100 iterations, The $Z_{\max}$ achieved is 0.2993and the corresponding values of the optimum input parameters are:

Spray distance: 75 mm,

Carrier Gas Flow: 40 Lit./min,
Powder flow rate: 25 Gms./min,
RPM of the substrate: 150 rpm,
Arc current: 500 A.

These input parameter values are simultaneously satisfying all the three objectives considered for Al_2O_3-40% TiO_2 coating on EN24 substrate. The convergence graph of TLBO optimization process is shown as **Figure 7**.

The combined objective function is once again generated considering assumed weights, *i.e.*, $W_T = 0.50$, $W_R = 0.25$ and $W_H = 0.25$, and TLBO algorithm is applied on the combined objective function. The optimum value of coefficient Z_{max} is 0.0230and the corresponding values of optimum input parameters are:

Spray distance: 175 mm,
Carrier Gas Flow: 40 Lit./min,
Powder flow rate: 50 Gms./min,
RPM of the substrate: 350 rpm,
Arc current: 500 A.

From the convergence data of TLBO, it is concluded that there is a drastic change in the optimum input parameters derived, while changing the weights of individual objective function from AHP based one to equal weights. Two parameters, "Spray distance", "substrate rpm" and "powder flow rate" are shifting from minimum to maximum in the case of equal weights. The convergence graph of TLBO is shown as **Figure 8**.

4. Conclusion

Research work in field of ceramic coating on EN4 alloy steel is rarely seen. In the field of surface coating with Al_2O_3-40% TiO_2, mathematical modeling and optimization are also very rare. In the present work, regression analysis is used to generate mathematical models for all the output parameters. The confirmation tests are carried out

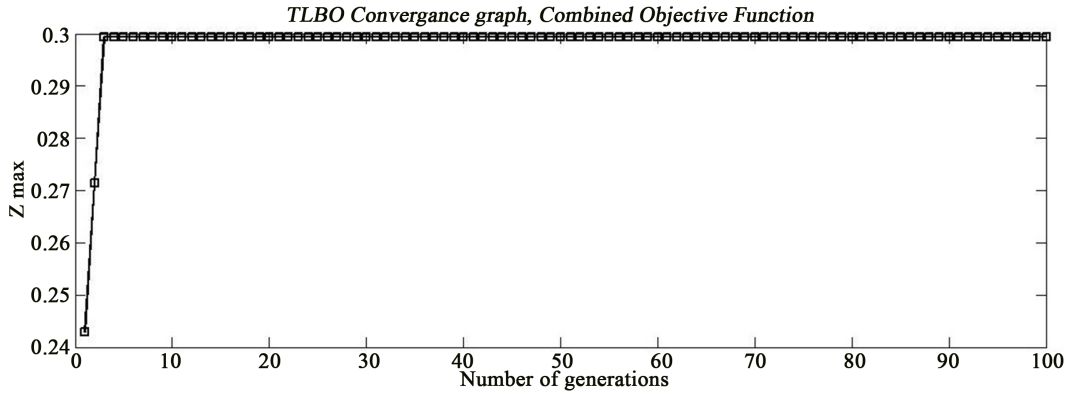

Figure 7. Convergence graph of TLBO for the combined objective function.

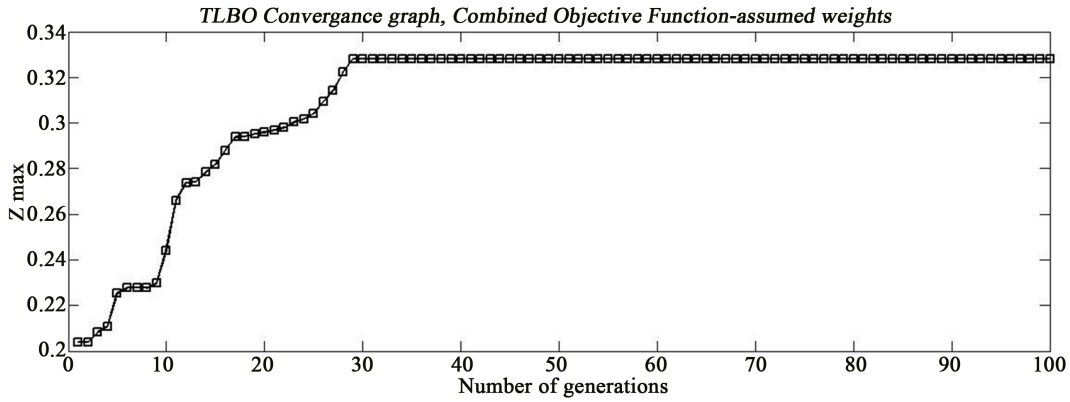

Figure 8. Convergence graph of TLBO for combined objective function with equal weights of objectives.

and have given near about the same values, in comparison to the predicted values and the % of error is negligible. TLBO algorithm, which is a latest advanced optimization technique, is used to carry out the optimization. A combined objective function is generated using apriori method. The combined objective function is successfully optimized using TLBO algorithm to obtain the global optimum values for input parameters. TLBO algorithm has proven its simplicity and its practical ability to solve the multi objective optimization problems effectively. The weights of individual objective functions of output parameters in the combined objective function is decided by AHP method which takes into account the preferences of the researcher during decision making. SN analyses are carried out to reveal the dominance of the process input parameters on each of the output parameters. The input parameters variation directly affects the characteristics of output parameters. Huge number of input as well as output parameters can be easily optimized using the current approach and the same can be applied to any type of substrates. Optimization problems related to HVOF, cold spraying, hard chrome coating, nirtiding and carbide coating can be effectively solved by applying the same method.

References

[1] Ramachandran, C.S., Balasubramanian, V., Ananthapadmanabhan, P.V. and Viswabaskaran, V. (2012) Influence of Intermixed Interfacial Layers in the Thermal Cycling Behaviour of Atmospheric Plasma Sprayed Lanthanum Zirconate Based Coating. *Ceramics International*, **38**, 4081-4096. http://dx.doi.org/10.1016/j.ceramint.2012.01.066

[2] Yang, Y., Wang, Y., Tian, W., Yan, D.R., Zhang, J.X. and Wang, L. (2015) Influence of Composite Powders' Microstructure on the Microstructure and Properties of Al2O3-TiO2 Coatings Fabricated by Plasma Spraying. *Materials and Design*, **65**, 814-822. http://dx.doi.org/10.1016/j.matdes.2014.09.078

[3] Forghani, S.M., Ghazali, M.J., Muchtar, A., Daud, A.R., Yusoff, N.H.N. and Azhari, C.H. (2013) Effects of Plasma spray Parameters on TiO_2-Coated Mild Steel Using Design of Experiment (DoE) Approach. *Ceramics International*, **39**, 3121-3127. http://dx.doi.org/10.1016/j.ceramint.2012.09.092

[4] Kang, J.J., Xu, B.S., Wang, H.D. and Wang, C.B. (2014) Influence of Contact Stress on Rolling Contact Fatigue of Composite Ceramic Coatings Plasma Sprayed on a Steel Roller. *Tribology International*, **73**, 47-56. http://dx.doi.org/10.1016/j.triboint.2013.12.019

[5] Mishra, N.K., Mishra, S.B. and Kumar, R. (2014) Oxidation Resistance of Low-Velocity Oxy Fuel-Sprayed Al_2O_3-13TiO_2 Coating on Nickel-Based Superalloys at 800℃. *Surface and Coating Technology*, **260**, 23-27. http://dx.doi.org/10.1016/j.surfcoat.2014.07.089

[6] Bolleddu, V., Racherla, V. and Bandyopadhyay, P.P. (2014) Microstructural and Tribological Characterization of Air Plasma Sprayed Nanostructured Alumina-Titania Coatings Deposited with Nitrogen and Argon as Primary Plasma Gases. *Materials and Design*, **59**, 252-263. http://dx.doi.org/10.1016/j.matdes.2014.02.040

[7] Morks, M.F. and Akimoto, K. (2008) The Role of Nozzle Diameter on the Microstructure and Abrasionwear Resistance of Plasma Sprayed Al_2O_3/TiO_2 Composite Coatings. *Journal of Manufacturing Processes*, **10**, 1-5. http://dx.doi.org/10.1016/j.jmapro.2008.10.001

[8] Yugeswaran, S., Selvarajan, S.V., Vijay, M., Ananthapadmanabhan, P.V. and Sreekumar, K.P. (2010) Influence of Critical Plasma Spraying Parameter (CPSP) on Plasma Sprayed Alumina-Titania Composite Coatings. *Ceramics International*, **36**, 141-149. http://dx.doi.org/10.1016/j.ceramint.2009.07.012

[9] Palacio, C.C., Agiorges, H., Vargas, F. and Diaz, A.F. (2013) Effect of Mechanical Properties on Drilling Resistance of Al_2O_3-TiO_2 Coating Manufactured by Atmospheric Plasma Spraying. *Surface and Coatings Technology*, **220**, 144-146. http://dx.doi.org/10.1016/j.surfcoat.2012.10.075

[10] Rico, A., Poza, P. and Rodriguez, J. (2013) High Temperature Tribological Behavior of Nanostructured and Conventional Plasma Sprayed Alumina-Titania Coatings. *Vacuum*, **88**, 149-154. http://dx.doi.org/10.1016/j.vacuum.2012.01.008

[11] Wang, C., Lan, L., Fan, J., Zhang, D. and Wang, H. (2013) Effect of Spraying Power on Microstructure and Properties of Supersonic Plasma Sprayed Al_2O_3 Coating on Porous Si_3N_4 Substrate. *Journal of Alloy and Compounds*, **569**, 152-157. http://dx.doi.org/10.1016/j.jallcom.2012.12.097

[12] Vargas, F., Agiorges, S., Fauchais, P., Lopez, M.E. and Calderon, J.A. (2013) Permeation of Saline Solution Al_2O_3-TiO_2 Coatings Elaborated by Atmospheric Plasma Spraying. *Surface and Coatings Technology*, **220**, 85-89. http://dx.doi.org/10.1016/j.surfcoat.2012.11.038

[13] Znamirowiski, Z., Nitsch, K. and Pawtowski, L. (2013) The Electric Charge Transport in Titania-Alumina Composite Cold Cathodes Made Using Atmospheric Plasma Spraying and Laser Engraving. *Surface and Coatings Technology*, **220**, 271-275. http://dx.doi.org/10.1016/j.surfcoat.2013.01.002

[14] Vicent, M., Bannier, E., Benavente, R., Salvador, M.D., Molina, T., Moreno, R. and Sanchez, E. (2013) Influence of

the Feedstock Characteristics on the Microstructure and Properties of Al_2O_3-TiO_2 Plasma Sprayed Coating. *Surface and Coatings Technology*, **220**, 74-79. http://dx.doi.org/10.1016/j.surfcoat.2012.09.042

[15] Murakami, Y., Kawakami, K. and Duckworth, W.E. (1991) Quantitative Evaluation of Effects of Shape and Size of Artificially Introduced Alumina Particles on the Fatigue Strength of (EN24) Steel. *International Journal of Fatigue*, **13**, 489-499. http://dx.doi.org/10.1016/0142-1123(91)90485-H

[16] Ramesh, R. and Gnanamoothy, R. (2006) Fretting Wear Behavior of Liquid Nitrided Structural Steel, En24 and Bearing Steel, En31. *Journal of Materials Processing Technology*, **171**, 61-67. http://dx.doi.org/10.1016/j.jmatprotec.2005.06.048

[17] Sarmah, B.P. and Khare, M.K. (1988) Some Investigations of the Wear Mechanisms of Widalon Carbide Inserts in Machining EN24 Steel. *Wear*, **127**, 229-240. http://dx.doi.org/10.1016/0043-1648(88)90157-3

[18] Tomlinson, W.J., Blunt, L.A. and Spraggett, S. (1988) Running-In Wear of White Layers Formed on EN24 Steel by Centreless Grinding. *Wear*, **128**, 83-91. http://dx.doi.org/10.1016/0043-1648(88)90254-2

[19] Aparnadevi, I., Sudhakar, I. and Venkata Ramana, V.S.N. (2015) An Experimental Study on Corrosion Behavior of EN8 and EN24 Grade Steels. *Materials Today*: *Proceedings*, **2**, 1251-1256. http://dx.doi.org/10.1016/j.matpr.2015.07.039

[20] Ghosh, S., Yadav, S. and Das, G. (2008) Ball Indentation Technique: A Currently Developed Tool to Study the Effect of Various Heat Treatments on the Mechanical Properties of EN24 Steel. *Materials Letters*, **62**, 3966-3968. http://dx.doi.org/10.1016/j.matlet.2008.05.048

[21] Mohandas, K.N., Ramesh, C.S., Eshwara Prasad, K. and Balashanmugam, N. (2014) Study of the Surface Integrity and Heat Measurement of Hard Turning of Hard Chrome Coated EN24 Substrate. *Procedia Materials Science*, **5**, 1947-1956. http://dx.doi.org/10.1016/j.mspro.2014.07.527

[22] Troczynski, T. and Plamondon, M. (1992) Response Surface Methodology for Optimization of Plasma Spraying. *Journal of Thermal Spray Technology*, **1**, 293-300. http://dx.doi.org/10.1007/BF02647156

[23] Steeper, T.J., Varacalle, D.J., Wilson, G.C., Riggs, W.L., Rotolico, A.J. and Nerz, J.A. (1993) A Design of Experiment Study of Plasma-Sprayed Alumina-Titania Coatings. *Journal of Thermal Spray Technology*, **2**, 251-256. http://dx.doi.org/10.1007/BF02650473

[24] Pierlot, C., Pawlowski, L., Bigan, M. and Chagnon, P. (2008) Design of Experiments in Thermal Spraying: A Review. *Surface and Coatings Technology*, **202**, 4483-4490. http://dx.doi.org/10.1016/j.surfcoat.2008.04.031

[25] Li, H.K., Li, C.X., Chen, K.X. and Zhang, Z.J. (2002) Investigation of Optimal Control System for Plasma Arc Spraying. *China Welding Institute*, **2**, 9-12.

[26] Rao, R.V., Savsani, V.J. and Vakharia, D.P. (2011) Teaching-Learning-Based Optimization: A Novel Method for Constrained Mechanical Design Optimization Problems. *Computer-Aided Design*, **43**, 303-315. http://dx.doi.org/10.1016/j.cad.2010.12.015

[27] Rao, R.V. (2015) Teaching Learning Based Optimization Algorithm and Its Engineering Applications. Springer International Publishing, Switzerland.

[28] Rao, R.V. (2016) Jaya: A Simple and New Optimization Algorithm for Solving Constrained and Unconstrained Optimization Problems. *International Journal of Industrial Engineering Computations*, **7**, 19-34.

[29] Pickard, J., Carretaro, J.A. and Bhavsar, V.C. (2016) On the Convergence and Origin Bias of the Teaching-Learning-Based-Optimization Algorithm. *Applied Soft Computing*, **46**, 115-127. http://dx.doi.org/10.1016/j.asoc.2016.04.029

[30] Rao, R.V. and Patel, V. (2013) Comparative Performance of an Elitist Teaching-Learning-Based Optimization Algorithm for Solving Unconstrained Optimization Problems. *International Journal of Industrial Engineering Computations*, **4**, 29-50. http://dx.doi.org/10.5267/j.ijiec.2012.09.001

[31] Rao, R.V. and Patel, V. (2012) An Elitist Teaching-Learning-Based Optimization Algorithm for Solving Complex Constrained Optimization Problems. *International Journal of Industrial Engineering Computations*, **3**, 535-560. http://dx.doi.org/10.5267/j.ijiec.2012.03.007

[32] Rao, R.V. (2015) Review of Applications of TLBO Algorithm and a Tutorial for Beginners to Solve the Unconstrained and Constrained Optimization Problem. *Decision Science Letters*, **5**, 1-30.

[33] Saaty, T.L. (2000) Fundamentals of the Analytic Hierarchy Process. RWS Publications, Pittsburgh.